

## Analytical Method for Predicting Ferromagnetic Properties of Benzyl-Radical Polymers Based on NBMO Theory

Yuuichi Orimoto<sup>†</sup> and Yuriko Aoki<sup>\*,†,‡</sup>

*Department of Material Sciences, Faculty of Engineering Sciences, Kyushu University, 6-1 Kasuga-Park, Fukuoka 816-8580, Japan, and Group, PRESTO, Japan Science and Technology Agency (JST), Kawaguchi Center Building, 4-1-8 Honcho, Kawaguchi, Saitama 332-0012, Japan*

Received January 5, 2006

**Abstract:** It has been demonstrated that the high-spin stability of benzyl radical oligomers can be predicted without any quantum chemical calculations. This method is composed of three steps: (1) predicting the shapes of nonbonding molecular orbitals (NBMOs), (2) counting up the mixings of NBMOs, and (3) formulating the mixings for the number of radical centers ( $N$ ). This treatment enables us to predict the high-spin stability evaluated by ab initio MO calculations involving the post-Hartree–Fock method or the density functional theory (DFT) method.

### 1. Introduction

Recently, experimental interests in organic magnets have been roughly classified into two types: the synthesis of crystalline solids composed of small radical molecules or charge-transfer salts<sup>1,2</sup> and that of organic  $\pi$ -conjugated systems.<sup>3–8</sup> In particular, high-spin  $\pi$ -conjugated systems have received growing interest as new organic magnets. This is because high transition temperature is theoretically predicted for the  $\pi$ -conjugated systems due to a strong exchange interaction between radicals through  $\pi$ -conjugated networks.<sup>3,9</sup> In 2001, Rajca et al. actually succeeded in the synthesis of ultrahigh-spin  $\pi$ -conjugated polymers with spin quantum numbers ( $S$ ) > 5000.<sup>6</sup> Numerous attempts have been made to explain the ferromagnetism in  $\pi$ -conjugated systems both experimentally<sup>3–8,10–13</sup> and theoretically.<sup>14–17</sup> Borden et al. conducted a molecular orbital (MO) approach to clarify the relationship between exchange interactions and ferromagnetic properties in organic conjugated systems.<sup>18–20</sup>

As another MO approach to predict ferromagnetism, one of the authors, Aoki et al., proposed a simple method to estimate the ferromagnetic properties of  $\pi$ -conjugated sys-

tems based on the  $L_{ij}^{\min}$  value, which corresponds to the mixing between nonbonding molecular orbitals (NBMOs).<sup>21</sup>

In the NBMOs of alternant hydrocarbon systems, the carbon atoms with MO coefficients can be defined as active atoms (denoted by “\*”), and the other carbon atoms with no coefficients can be defined as inactive atoms (denoted by “0”). When an allyl radical molecule is considered as a NBMO unit, there are two types of linkages between two NBMO units (see Figure 1 in ref 21). One is a (0–0) linkage that connects two inactive carbons. The other is a (0–\*) linkage that connects an inactive carbon to an active carbon. In both types of linkages, two degenerated levels of NBMOs are obtained. In the (0–0) linkage, the NBMO level of each unit is preserved in the entire system because there is no interaction between the inactive carbon atoms. Thus, the (0–0) linkage corresponds to a “disjoint” type linkage. In contrast, in the (0–\*) linkage, the energy levels of the NBMOs are preserved because of the interaction between the inactive and active carbon atoms (see Figure 3 in ref 21). The (0–\*) linkage corresponds to a “nondisjoint” type linkage. That is to say, the two types of interactions that correspond to the stabilization and destabilization of the orbitals are canceled out by each other according to the pairing theorem<sup>22</sup> within the framework of the simple Hückel method. Our previous paper<sup>21</sup> used algebraic equations to prove that these two types of linkages, (0–0) and (0–\*), do not change the eigenvalues of the NBMOs.

\* Corresponding author e-mail: aoki@cube.kyushu-u.ac.jp.

<sup>†</sup> Kyushu University.

<sup>‡</sup> Group, PRESTO, Japan Science and Technology Agency (JST).

A new value

$$L_{ij} = \sum_r (C_{ir} C_{jr})^2 \quad (1)$$

was proposed by Aoki et al. to estimate the mixing between NBMOs for the prediction of the high-spin stability in “nondisjoint” type systems,<sup>21</sup> where  $C_{ir}$  is the coefficient of AO  $\chi_r$  in the  $i$ th NBMO. In general, we can change the MO coefficients of degenerated NBMOs by using a unitary transformation (see Figure 2 in ref 21). Therefore, the stability of the high-spin ground state can be predicted by the smallest  $L_{ij}$  value, i.e., the  $L_{ij}^{\min}$  value, after the unitary transformation. When  $L_{ij}$  has the smallest value, NBMO coefficients are selected to minimize the mixing between  $i$ th and  $j$ th NBMOs.

The total energy difference between excited singlet and triplet states at the Hartree–Fock MO level is expressed as

$$2K_{ij} = E(S) - E(T) \quad (2)$$

where  $E(S)$  and  $E(T)$  denote total energies in excited singlet and triplet states, respectively. The  $K_{ij}$  is the exchange integral between  $i$ th and  $j$ th NBMOs, that is

$$K_{ij} = \sum_r \sum_s \sum_t \sum_u C_{ir} C_{js} C_{it} C_{ju} (rs|tu) \quad (3)$$

where  $r, s, t$ , and  $u$  indicate atomic orbitals (AOs).  $C_{ir}$  is the coefficient of AO  $\chi_r$  in the  $i$ th NBMO in the linear combination of AO (LCAO) approximation. The two-electron integral  $(rs|tu)$  in eq 3 is expanded by

$$(rs|tu) = \int \int \chi_r(1) \chi_s(1) \frac{1}{r_{12}} \chi_t(2) \chi_u(2) d\tau_1 d\tau_2 \quad (4)$$

When the 2-electron integrals part of  $K_{ij}$  is approximated by a one-center two-electron integral, e.g.,  $(rr|rr)$ ,  $\sum_r (C_{ir} C_{jr})^2 (rr|rr)$  can be obtained from eq 3. Therefore, the  $L_{ij}$  value in eq 1 corresponds to the MO coefficients part of the one-center two-electron terms in eq 3 and corresponds to the exchange integral ( $K_{ij}$ ) as well as the high-spin stability expressed by eq 2. Because the  $L_{ij}$  is composed of only MO coefficients, we can efficiently examine the stability of high-spin ground state by calculating the  $L_{ij}^{\min}$  value using various methods from a simple Hückel method to an ab initio MO method after unitary transformation.

Although the  $L_{ij}^{\min}$  value is useful for evaluating the ferromagnetic properties of NBMO systems, there are some problems with huge systems in which we cannot obtain coefficients of the whole MO. The purpose of this article is to predict the  $L_{ij}^{\min}$  value analytically without performing any quantum chemical calculations and unitary transformations. Our new treatment enables us to predict the shapes of the NBMOs corresponding to the  $L_{ij}^{\min}$  value by using a “zero sum rule” in the NBMO theory. In the present article, we focused on benzyl radical type systems as a first step of the analysis, because the benzyl radical unit is involved in typical organic ferromagnetic materials. It was found that we were able to predict the  $L_{ij}^{\min}$  values of various types of benzyl radical type oligomers without using direct calculations.

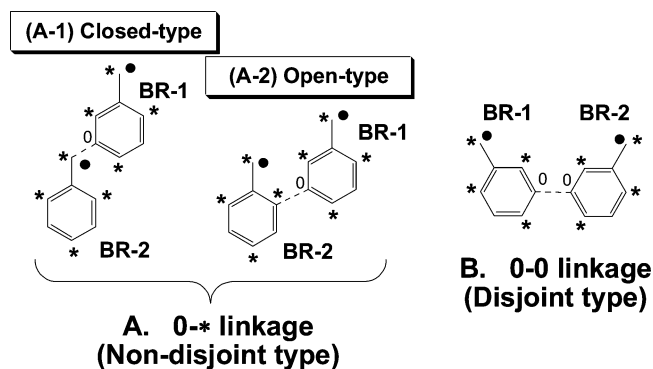


**Figure 1.** 0-\* and 0–0 linkages between benzyl radical (BR) units in the benzyl radical dimer model. The broken line denotes the C–C bond connecting the BR units.

## 2. Method

**2.1. Benzyl Radical Dimer Model.** The benzyl radical dimer model in Figure 1 is composed of two benzyl radical (BR) units, BR-1 and BR-2. It should be noted that the structure of the benzyl radical oligomer in the present article is assumed to have a planar structure. According to the classification mentioned above, we can divide benzyl radical dimer models into two types: (A) nondisjoint type with a (0-\*) linkage and (B) disjoint type with a (0–0) linkage. Furthermore, the former type is divided into “(A-1) closed-type” and “(A-2) open-type.” The nondisjoint closed-type model, (A-1), is defined as a model in which two BR units are connected at the sites of the inactive carbon atom (0) in the meta position of BR-1 and the radical center of BR-2. Here, the radical center is defined as the active carbon atom (\*) having the largest NBMO coefficient in the BR unit marked by a dot. In contrast, the nondisjoint open-type model, (A-2), is defined as the model that includes the connection between the inactive atom (0) in the meta position of BR-1 and the active atom (\*) in the ortho position of BR-2. In the present work, only the nondisjoint closed-type model, (A-1), is focused on, because we have not yet succeeded in predicting the ferromagnetic properties for the open-type model.

Figure 2 shows a method for predicting the shapes of NBMOs that provide the  $L_{ij}^{\min}$  value for a benzyl radical dimer model. This procedure is the first step of the analytical prediction (AP) method to evaluate the high-spin stability of nondisjoint closed-type benzyl radical oligomers. Because the benzyl radical dimer model in Figure 2 has a (0-\*) linkage, the system keeps two degenerated NBMOs unchanged as a result of the interaction between the inactive and active carbon atoms. The procedures are summarized as follows:

(i) In the first step (see step 0 in Figure 2), the whole system is divided into two radical units, BR-1 and BR-2.

(ii) Next, we focus on the upper BR unit (BR-1) and consider assigning its NBMO coefficients using the letter “a” according to the conventional NBMO rule<sup>23,24</sup> (step 1a). Furthermore, another unit (BR-2) should be assigned based on the NBMO coefficients of BR-1 (step 2a). According to the “zero sum rule” in the NBMO theory, the NBMO

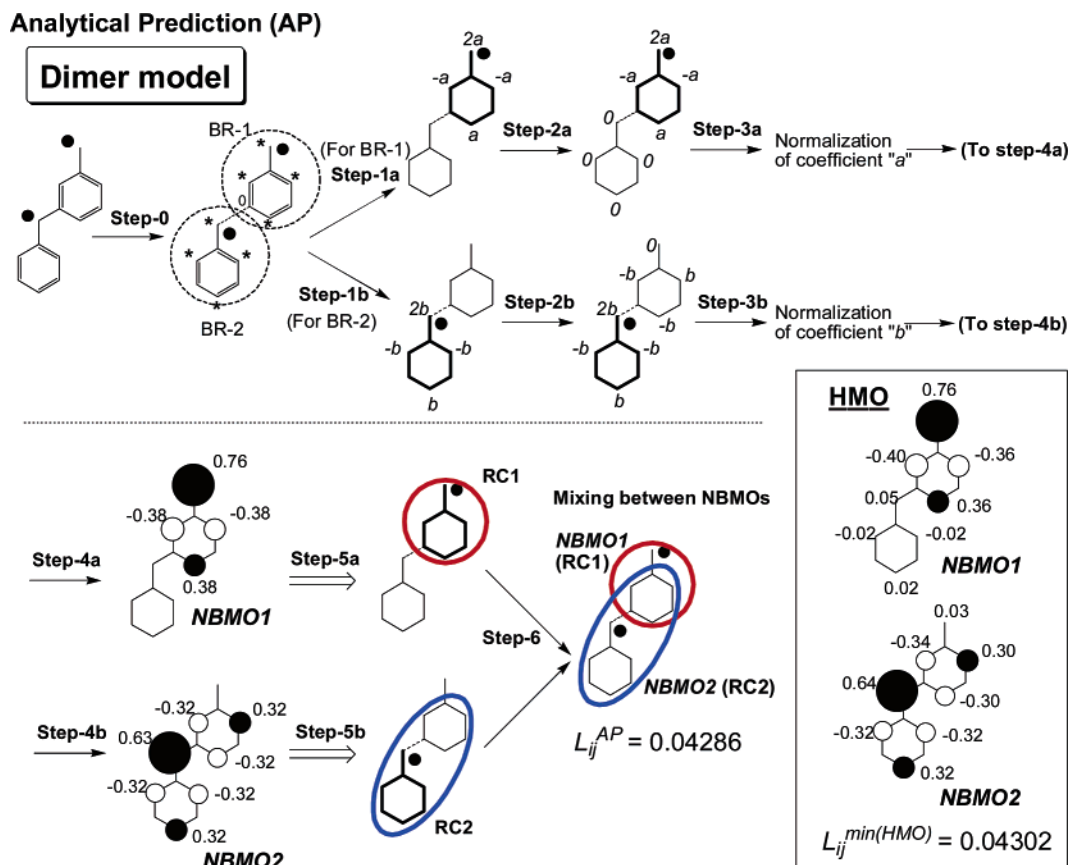


**Figure 2.** Procedures for predicting the shapes of NBMOs and the  $L_{ij}$  values by the analytical prediction (AP) method. The benzyl radical units under consideration are indicated by bold lines. The results by the simple Hückel method (HMO) are shown in the rectangular box.

coefficients of all the carbon atoms in BR-2 become zero. This implies that the NBMO coefficients of BR-1 cannot be delocalized over the region of BR-2.

(iii) Conversely, we focus on the lower BR unit (BR-2) and consider assigning the NBMO coefficients by using the letter "b" (step 1b), followed by assigning the NBMO coefficients of the BR-1 region (step 2b). In this case, one can assign the BR-1 region with nonzero NBMO coefficients except for the site of the radical center in BR-1. Thus, the NBMO coefficients of BR-2 can be delocalized over the region of BR-1 through a C–C bond connecting two BR units (broken line), and the NBMO spreads over two benzene rings.

(iv) The "a" and "b" are normalized for each NBMO by  $\sum_r C_{ir}^2 = 1$

$$\text{Step 3a: } (2a)^2 + 2(-a)^2 + a^2 = 7a^2 = 1;$$

$$a = \frac{1}{\sqrt{7}} \approx 0.37796 \quad (5a)$$

$$\text{Step 3b: } (2b)^2 + 4(-b)^2 + 2b^2 = 10b^2 = 1;$$

$$b = \frac{1}{\sqrt{10}} \approx 0.31623 \quad (5b)$$

(v) Finally, we obtained NBMO1 and NBMO2 (see steps 4a and 4b). Here, we assigned the types of radical centers (RCs) according to the NBMO shape. In NBMO1, MO

coefficients spread over one benzene ring (step 5a). In NBMO2, MO coefficients spread over two benzene rings (step 5b). The radical centers that belong to NBMO1 and NBMO2 are called RC1 and RC2, respectively.

(vi) The stability of the high-spin ground state is predicted by calculating the mixing between the two NBMOs (see step 6), i.e.,  $L_{ij}^{AP} = \sum_r (C_{ir}C_{jr})^2$ , by

$$L_{ij}^{AP} = L_{ij}^{AP[NBMO1(RC1)-NBMO2(RC2)]} = (ab)^2 + (ab)^2 + (ab)^2 =$$

$$3a^2b^2 = 3\left(\frac{1}{\sqrt{7}}\right)^2\left(\frac{1}{\sqrt{10}}\right)^2 = \frac{3}{70} \approx 0.04286 \quad (6)$$

where  $L_{ij}^{AP[NBMO1(RC1)-NBMO2(RC2)]}$  represents the mixing between NBMO1(RC1) and NBMO2(RC2).

Figure 2 also shows the calculation of NBMO coefficients by the simple Hückel method (HMO) and the  $L_{ij}^{min}$  value after unitary transformation ( $L_{ij}^{min(HMO)} = 0.04302$ ). It was found that the difference in the NBMO coefficients between the AP and HMO methods is very small. Therefore, the  $L_{ij}^{AP}$  value agreed well with the  $L_{ij}^{min(HMO)}$  value and provides an even better minimum value in  $L_{ij}$ . In the present case, it was found that the  $L_{ij}^{min(HMO)}$  value is slightly larger than the  $L_{ij}^{AP}$  value. This is because the NBMO coefficients calculated by the HMO method are not suitable for the benzyl radical dimer model as the initial coefficients for unitary rotation, and thus NBMO coefficients do not lead to the minimum  $L_{ij}$  value

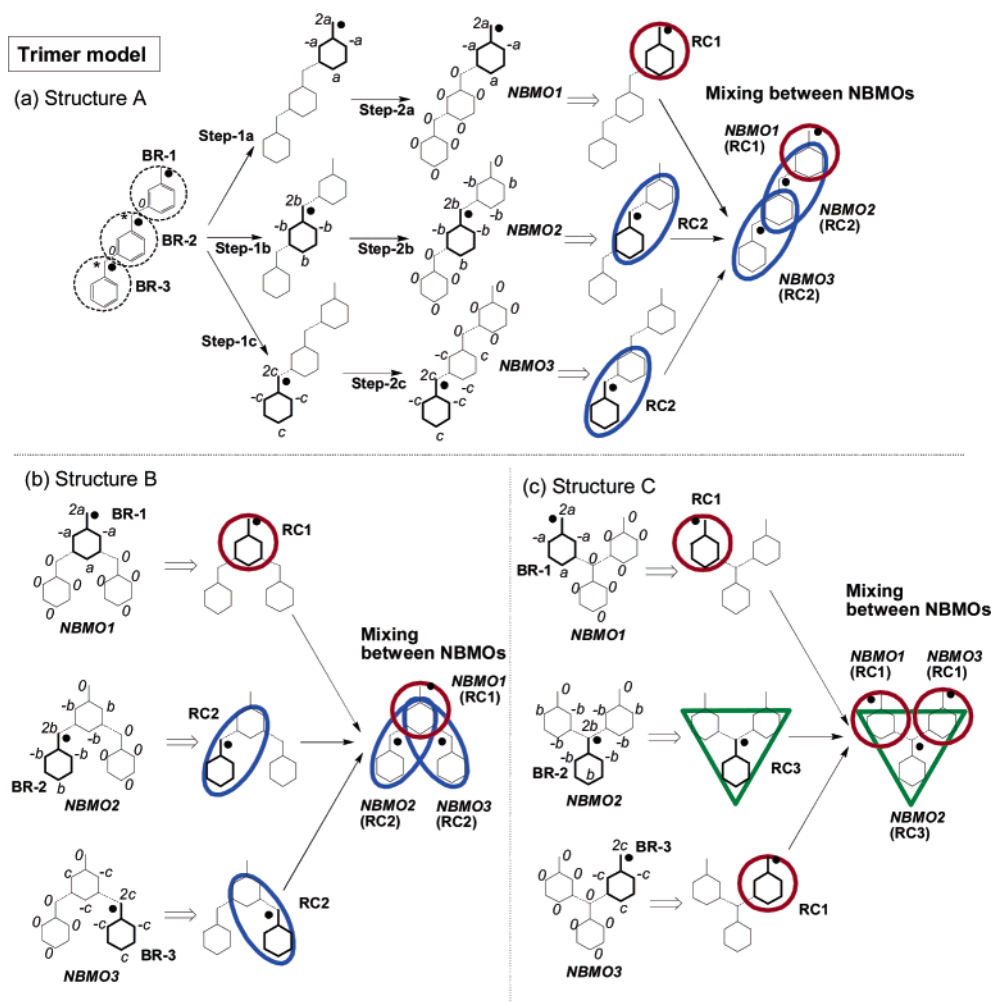


**Figure 3.** Analytical prediction of the  $L_{ij}$  value for three different structures, A–C in the benzyl radical trimer model. The benzyl radical units under consideration are indicated by bold lines.

after unitary transformation. This means that the  $L_{ij}^{\text{AP}}$  value estimated by the AP method provides us with the minimum value of  $L_{ij}$  regardless of the systems.

**2.2. Benzyl Radical Trimer Model.** The benzyl radical trimer model in Figure 3 is composed of three BR units (BR-1, BR-2, and BR-3). For the “nondisjoint closed-type” trimer model, we consider three types of structures A, B, and C with three NBMOs. We can predict the shapes of the NBMOs in the same way that we can predict the benzyl radical dimer model mentioned above.

Structure A is considered first (see Figure 3(a)). NBMO coefficients are assigned for each BR unit under consideration (steps 1a–c). Next, we consider the coefficients of each NBMO for the whole system (steps 2a–c), followed by normalization of the NBMO coefficients. The letters “a”, “b”, and “c” are used for the MO coefficients of NBMO1, NBMO2, and NBMO3, respectively. According to subsection 2.1, one can assign NBMO1, NBMO2, and NBMO3 as RC1, RC2, and RC2, respectively. In a manner similar to the procedure (iv) in subsection 2.1, these NBMO coefficients are calculated with  $a = 1/\sqrt{7}$  (for RC1) and  $b = c = 1/\sqrt{10}$  (for RC2). Therefore, the  $L_{ij}^{\text{AP}}$  value for structure A can be evaluated by

$$\begin{aligned} \text{Structure A: } L_{ij}^{\text{AP}} &= L_{ij}^{\text{AP}[\text{NBMO1(RC1)}-\text{NBMO2(RC2)}]} + \\ &L_{ij}^{\text{AP}[\text{NBMO2(RC2)}-\text{NBMO3(RC2)}]} = 3 \times (ab)^2 + 3 \times (bc)^2 = \\ &\frac{3}{70} + \frac{3}{100} \approx 0.07286 \quad (7) \end{aligned}$$

There is no mixing between NBMO1(RC1) and NBMO3(RC2) in structure A.

In structure B, NBMO1, NBMO2, and NBMO3 belong to RC1, RC2, and RC2, respectively (see Figure 3(b)). Thus, we obtained  $a = 1/\sqrt{7}$  (for RC1) and  $b = c = 1/\sqrt{10}$  (for RC2). The  $L_{ij}^{\text{AP}}$  value for B structure is calculated by

$$\begin{aligned} \text{Structure B: } L_{ij}^{\text{AP}} &= L_{ij}^{\text{AP}[\text{NBMO1(RC1)}-\text{NBMO2(RC2)}]} + \\ &L_{ij}^{\text{AP}[\text{NBMO1(RC1)}-\text{NBMO3(RC2)}]} + L_{ij}^{\text{AP}[\text{NBMO2(RC2)}-\text{NBMO3(RC2)}]} = \\ &3 \times (ab)^2 + 3 \times (ac)^2 + 3 \times (bc)^2 = \frac{3}{70} + \frac{3}{70} + \frac{3}{100} \approx \\ &0.11571 \quad (8) \end{aligned}$$

Finally, we consider structure C (see Figure 3(c)). Both NBMO1 and NBMO3 are assigned as RC1, and we obtained  $a = c = 1/\sqrt{7}$  (for RC1). The NBMO2 in which the coefficients spread over three benzene rings is assigned as



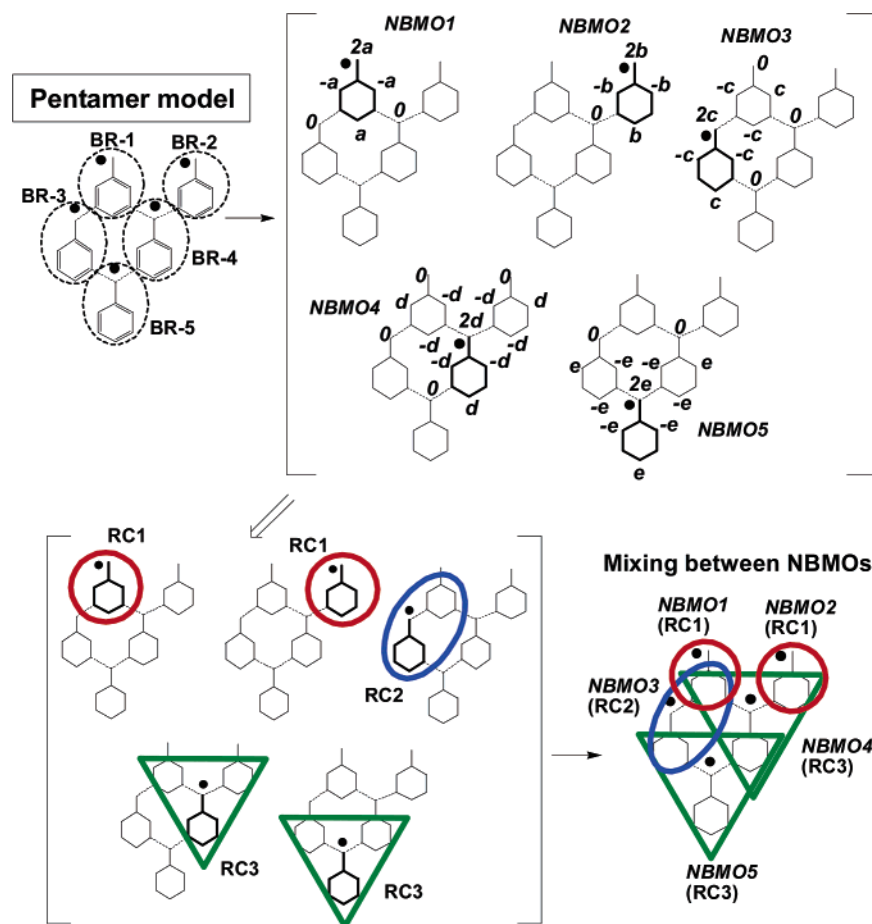


**Figure 4.** Analytical prediction of the  $L_{ij}$  value for a benzyl radical pentamer model. The benzyl radical units under consideration are indicated by bold lines.

RC3. The NBMO coefficients corresponding to RC3 are calculated by the normalization of value “ $b$ ” in Figure 3(c), i.e.

$$(2b)^2 + 6(-b)^2 + 3b^2 = 13b^2 = 1; b = \frac{1}{\sqrt{13}} \approx 0.27735 \quad (\text{for RC3}) \quad (9)$$

Therefore, the  $L_{ij}^{\text{AP}}$  value for structure C is calculated by

$$\begin{aligned} \text{Structure C: } L_{ij}^{\text{AP}} &= L_{ij}^{\text{AP[NBMO1(RC1)-NBMO2(RC3)]}} + \\ &L_{ij}^{\text{AP[NBMO2(RC3)-NBMO3(RC1)]}} = 3 \times (ab)^2 + 3 \times (bc)^2 = \\ &\frac{3}{91} + \frac{3}{91} \approx 0.06593 \quad (10) \end{aligned}$$

There is no mixing between NBMO1(RC1) and NBMO3(RC1) in structure C.

**2.3. Benzyl Radical Pentamer Model.** Figure 4 shows a benzyl radical pentamer model with five benzyl radical units, BR-1–BR-5. This model includes five NBMOs, NBMO1–NBMO5. NBMO1 and NBMO2 belong to RC1. NBMO3 corresponds to RC2, and both NBMO4 and NBMO5 correspond to RC3. Therefore, the NBMO coefficients are calculated with  $a = b = 1/\sqrt{7}$  (for RC1),  $c = 1/\sqrt{10}$  (for RC2), and  $d = e = 1/\sqrt{13}$  (for RC3). The  $L_{ij}^{\text{AP}}$  value can be estimated by

$$\begin{aligned} L_{ij}^{\text{AP}} &= L_{ij}^{\text{AP[NBMO1(RC1)-NBMO3(RC2)]}} + \\ &L_{ij}^{\text{AP[NBMO1(RC1)-NBMO4(RC3)]}} + L_{ij}^{\text{AP[NBMO2(RC1)-NBMO4(RC3)]}} + \\ &L_{ij}^{\text{AP[NBMO3(RC2)-NBMO4(RC3)]}} + L_{ij}^{\text{AP[NBMO3(RC2)-NBMO5(RC3)]}} + \\ &L_{ij}^{\text{AP[NBMO4(RC3)-NBMO5(RC3)]}} = 3 \times (ac)^2 + 3 \times (ad)^2 + 3 \times \\ &(bd)^2 + 3 \times (cd)^2 + 3 \times (ce)^2 + 3 \times (de)^2 = \\ &\frac{3}{70} + \frac{3}{91} + \frac{3}{91} + \frac{3}{130} + \frac{3}{130} + \frac{3}{169} \approx 0.17270 \quad (11) \end{aligned}$$

All the other combinations between the NBMOs in eq 11, for example, between NBMO1 and NBMO2, have no mixing.

**2.4. Treatment of Methylene or Methylidyne Radical Units.** Figure 5 shows a nondisjoint closed-type system including methylene ( $:\text{CH}_2$ ) or methylidyne ( $:\text{CH}^\bullet$ ) radical (MR) units, MR-1 and MR-2, in addition to benzyl radical units, BR-1 and BR-2. We can predict the shapes of the NBMOs and the  $L_{ij}^{\text{AP}}$  value for such a system in the following manner.

NBMO coefficients were assigned for each radical unit under consideration (see step 1). Note that the NBMO coefficient in the MR unit is initially assigned by “ $2a$ ” for MR-1 and “ $2c$ ” for MR-2. Next, we considered the coefficients of each NBMO in other radical units (see step 2) and obtained four NBMOs 1–4. NBMO1, 2, 3, and 4 can be assigned as RC1, RC1, RC2, and RC1, respectively (see step 3). After normalization of the NBMO coefficients,  $a =$

$b = d = 1/\sqrt{7}$  (for RC1) and  $c = 1/\sqrt{10}$  (for RC2) can be calculated. The  $L_{ij}^{AP}$  value is estimated (see step 4) by

$$L_{ij}^{AP} = L_{ij}^{AP[NBMO1(RC1)-NBMO2(RC1)]} + L_{ij}^{AP[NBMO1(RC1)-NBMO3(RC2)]} + L_{ij}^{AP[NBMO2(RC1)-NBMO3(RC2)]} + L_{ij}^{AP[NBMO3(RC2)-NBMO4(RC1)]} = 3 \times (ab)^2 + 3 \times (ac)^2 + 3 \times (bc)^2 + 3 \times (cd)^2 = \frac{3}{49} + \frac{3}{70} + \frac{3}{70} + \frac{3}{70} \approx 0.18980 \quad (12)$$

Therefore, we can treat methylene or methylidyne radical units in a manner similar to the benzyl radical units except for the initial assignment for the NBMO coefficients as shown in step 1 of Figure 5.

**2.5. Generalization of the Estimation of the  $L_{ij}^{AP}$  Value.** In the above subsections, we defined three types of radical centers according to the shape of their NBMOs. That is to say, RC1, RC2, and RC3 represent the NBMOs spreading over one benzene ring, two benzene rings, and three benzene rings, respectively. It should be noted that for a huge benzyl radical oligomer, only the three types of radical centers, RC1, RC2, and RC3, can be considered for a nondisjoint closed type system. Thus, only six types of mixings between the different shapes of  $i$ th and  $j$ th NBMOs are considered as

$$\text{RC1-RC1: } L_{ij}^{AP(RC1-RC1)} = 3 \times (\alpha_i^{RC1} \alpha_j^{RC1})^2 = 3 \times \left(\frac{1}{\sqrt{7}} \times \frac{1}{\sqrt{7}}\right)^2 = \frac{3}{49} \approx 0.06122 \quad (13a)$$

$$\text{RC1-RC2: } L_{ij}^{AP(RC1-RC2)} = 3 \times (\alpha_i^{RC1} \alpha_j^{RC2})^2 = 3 \times \left(\frac{1}{\sqrt{7}} \times \frac{1}{\sqrt{10}}\right)^2 = \frac{3}{70} \approx 0.04286 \quad (13b)$$

$$\text{RC1-RC3: } L_{ij}^{AP(RC1-RC3)} = 3 \times (\alpha_i^{RC1} \alpha_j^{RC3})^2 = 3 \times \left(\frac{1}{\sqrt{7}} \times \frac{1}{\sqrt{13}}\right)^2 = \frac{3}{91} \approx 0.03297 \quad (13c)$$

$$\text{RC2-RC2: } L_{ij}^{AP(RC2-RC2)} = 3 \times (\alpha_i^{RC2} \alpha_j^{RC2})^2 = 3 \times \left(\frac{1}{\sqrt{10}} \times \frac{1}{\sqrt{10}}\right)^2 = \frac{3}{100} = 0.03 \quad (13d)$$

$$\text{RC2-RC3: } L_{ij}^{AP(RC2-RC3)} = 3 \times (\alpha_i^{RC2} \alpha_j^{RC3})^2 = 3 \times \left(\frac{1}{\sqrt{10}} \times \frac{1}{\sqrt{13}}\right)^2 = \frac{3}{130} \approx 0.02308 \quad (13e)$$

$$\text{RC3-RC3: } L_{ij}^{AP(RC3-RC3)} = 3 \times (\alpha_i^{RC3} \alpha_j^{RC3})^2 = 3 \times \left(\frac{1}{\sqrt{13}} \times \frac{1}{\sqrt{13}}\right)^2 = \frac{3}{169} \approx 0.01775 \quad (13f)$$

where  $\alpha_i^{RC1}$  indicates the NBMO coefficient of  $i$ th NBMO with an RC1-type radical center. A series of NBMO coefficients is provided in subsections 2.1 and 2.2 as  $\alpha_i^{RC1} = \alpha_i^{RC1} = 1/\sqrt{7}$ ,  $\alpha_i^{RC2} = \alpha_i^{RC2} = 1/\sqrt{10}$ , and  $\alpha_i^{RC3} = \alpha_i^{RC3} = 1/\sqrt{13}$ . Therefore, the  $L_{ij}^{AP}$  value for the whole system

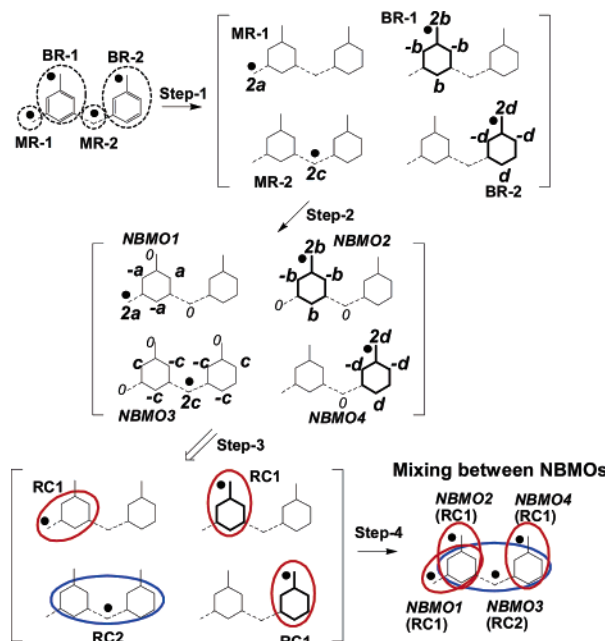


**Figure 5.** Analytical prediction of the  $L_{ij}$  value for a system including methylene ( $:\text{CH}_2$ ) or methylidyne ( $:\text{CH}^\bullet$ ) radical units. The benzyl radical units under consideration are indicated by bold lines.

can be calculated by counting all the NBMO mixings (eq 13a–f) over the whole system as

$$L_{ij}^{AP} = N^{AP(RC1-RC1)} L_{ij}^{AP(RC1-RC1)} + N^{AP(RC1-RC2)} L_{ij}^{AP(RC1-RC2)} + N^{AP(RC1-RC3)} L_{ij}^{AP(RC1-RC3)} + N^{AP(RC2-RC2)} L_{ij}^{AP(RC2-RC2)} + N^{AP(RC2-RC3)} L_{ij}^{AP(RC2-RC3)} + N^{AP(RC3-RC3)} L_{ij}^{AP(RC3-RC3)} \quad (14)$$

where  $N^{AP(RC1-RC1)}$ ,  $N^{AP(RC1-RC2)}$ , etc. indicate the number of mixings,  $L_{ij}^{AP(RC1-RC1)}$ ,  $L_{ij}^{AP(RC1-RC2)}$ , etc., respectively.

The process for counting the NBMO mixings can be conducted by judging whether the two NBMOs under consideration make mixings or not. For instance, for the benzyl radical pentamer model (see Figure 4) we can count the components of NBMO mixings using eqs 13 and 14 as

$$L_{ij}^{AP} = 0 \times L_{ij}^{AP(RC1-RC1)} + 1 \times L_{ij}^{AP(RC1-RC2)} + 2 \times L_{ij}^{AP(RC1-RC3)} + 0 \times L_{ij}^{AP(RC2-RC2)} + 2 \times L_{ij}^{AP(RC2-RC3)} + 1 \times L_{ij}^{AP(RC3-RC3)} = 1 \times \left(\frac{3}{70}\right) + 2 \times \left(\frac{3}{91}\right) + 2 \times \left(\frac{3}{130}\right) + 1 \times \left(\frac{3}{169}\right) \approx 0.17270 \quad (15)$$

Therefore, finally, we obtained the same results as eq 11. Similarly, one can count the NBMO mixings and calculate the  $L_{ij}^{AP}$  value for the system including methylene or methylidyne radical units.

### 3. Results and Discussion

Figure 6 shows model systems for a quasi-one-dimensional benzyl radical oligomer that are combined by the “nondisjoint closed-type”, as shown in Figure 1(A-1). Models 1–3 in

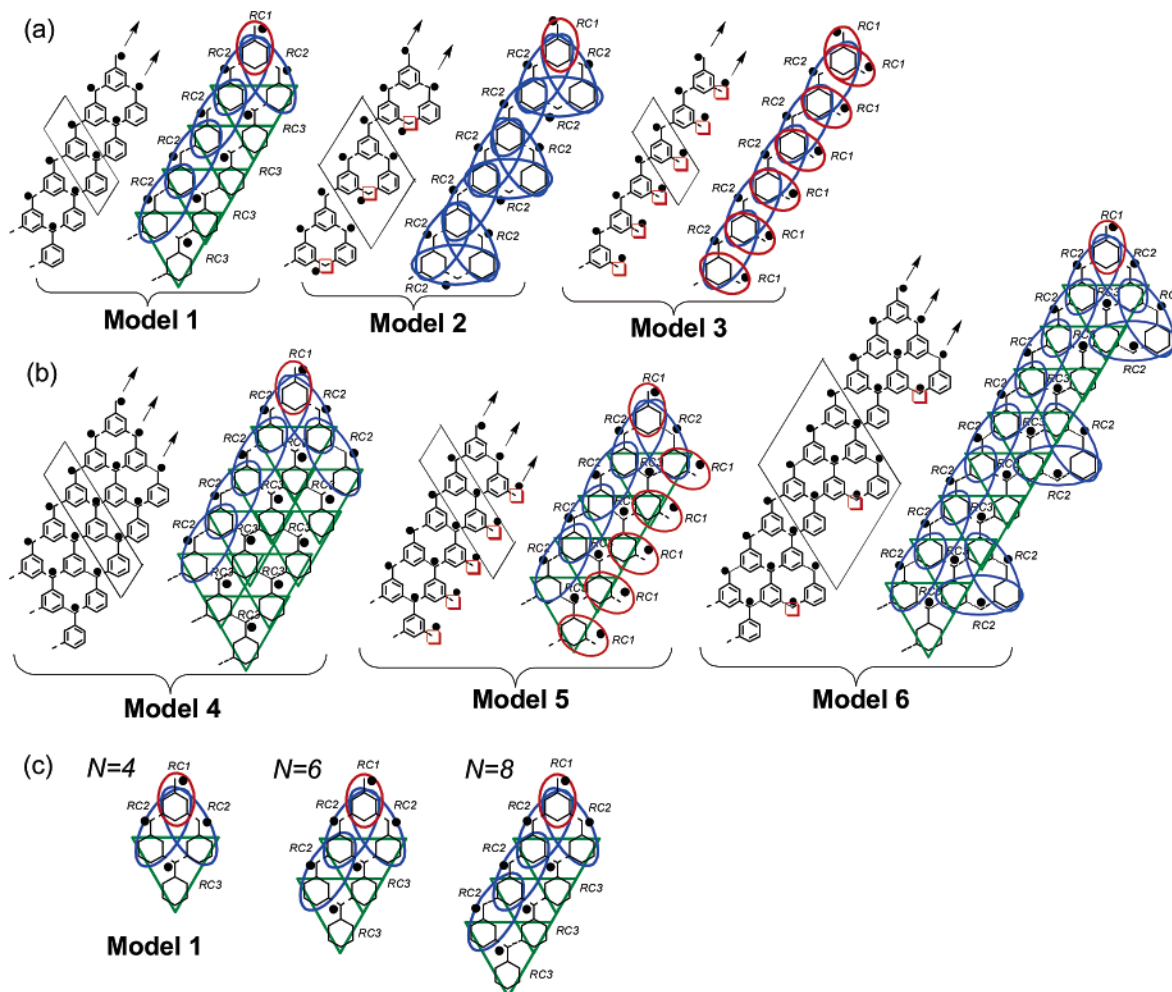


**Figure 6.** Nondisjoint closed-type models for quasi-one-dimensional benzyl radical oligomers with (a) two- and (b) three-line alignment of radical centers. The red open square indicates a methylene ( $\text{:CH}_2$ ) or methylidyne ( $\text{:CH}^*$ ) radical unit. The periodic structure for each system is shown in a parallelogram. The arrows indicate the directions of the alignment of the radical centers. The mixings between NBMOs are illustrated in the right-hand figure of each model. (c) Model 1 with  $N = 4, 6$ , and  $8$  for the formulation of the  $L_{ij}^{\text{AP}}$  value in Table 1.

Figure 6(a) correspond to “two-line systems” in which radical centers are arranged in two lines as shown by the arrows indicating the directions of alignment. In contrast, models 4–6 in Figure 6(b) correspond to “three-line systems” in which radical centers are arranged in three lines. Note that models 2, 3, 5, and 6 include methylene ( $\text{:CH}_2$ ) or methylidyne ( $\text{:CH}^*$ ) radical units as indicated by the red open squares in the figure.

**3.1. Analytical Predictions for Two-Line Systems.** In this subsection, we formulate the  $L_{ij}^{\text{AP}}$  value for the nondisjoint closed-type models 1–3 in the two-line system. When the number of radical centers is defined as “ $N$ ”, we can count the number of mixings between NBMOs according to the right figure of each model (see Figure 6(a)). Table 1 (a) and Figure 6(c) show the formulation of the  $L_{ij}^{\text{AP}}$  value for model 1. The number of  $L_{ij}^{\text{AP}}$ ’s components, that is,  $L_{ij}^{\text{AP(RC1-RC2)}}$ ,  $L_{ij}^{\text{AP(RC2-RC2)}}$ , etc., are counted for some sizes of periodic structures step by step ( $N = 4, 6, 8, \dots$ ). Eventually, we can estimate the number of each component for an arbitrary size of oligomer, that is,  $N = n$ . Therefore, for model 1 the  $L_{ij}^{\text{AP}}$  value is formulated as

$$\begin{aligned} \text{Model 1: } L_{ij}^{\text{AP}} &= 2L_{ij}^{\text{AP(RC1-RC2)}} + \left(\frac{N}{2} - 1\right)L_{ij}^{\text{AP(RC2-RC2)}} + \\ & (N - 2)L_{ij}^{\text{AP(RC2-RC3)}} + \left(\frac{N}{2} - 2\right)L_{ij}^{\text{AP(RC3-RC3)}} = \\ & \frac{6}{70} + \left(\frac{N}{2} - 1\right)\frac{3}{100} + (N - 2)\frac{3}{130} + \left(\frac{N}{2} - 2\right)\frac{3}{169} \quad (16a) \end{aligned}$$

where small “ $n$ ” is replaced with capital “ $N$ ”. The increase of the  $L_{ij}^{\text{AP}}$  value per radical center is calculated by considering the  $N$  limits ( $N \rightarrow \infty$ ) of  $L_{ij}^{\text{AP}}/N$  as

$$\begin{aligned} \lim_{N \rightarrow \infty} \frac{L_{ij}^{\text{AP}}}{N} &= \lim_{N \rightarrow \infty} \left\{ \frac{6}{70N} + \left(\frac{1}{2} - \frac{1}{N}\right)\frac{3}{100} + \left(1 - \frac{2}{N}\right)\frac{3}{130} + \right. \\ & \left. \left(\frac{1}{2} - \frac{2}{N}\right)\frac{3}{169} \right\} = \left(\frac{1}{2}\right)\frac{3}{100} + \frac{3}{130} + \left(\frac{1}{2}\right)\frac{3}{169} \approx 0.04695 \quad (16b) \end{aligned}$$

In a similar way, we can estimate the  $L_{ij}^{\text{AP}}$  values (see also Table 1(b) and (c)) and the increases per radical center for models 2 and 3 as follows:

$$\begin{aligned} \text{Model 2: } L_{ij}^{\text{AP}} &= 2L_{ij}^{\text{AP(RC1-RC2)}} + \\ & \left(\frac{7}{4}N - 4\right)L_{ij}^{\text{AP(RC2-RC2)}} = \frac{6}{70} + \left(\frac{7}{4}N - 4\right)\frac{3}{100} \quad (17a) \end{aligned}$$

$$\lim_{N \rightarrow \infty} \frac{L_{ij}^{AP}}{N} = \lim_{N \rightarrow \infty} \left\{ \frac{6}{70N} + \left( \frac{7}{4} - \frac{4}{N} \right) \frac{3}{100} \right\} = \left( \frac{7}{4} \right) \frac{3}{100} = 0.0525 \quad (17b)$$

**Model 3:**  $L_{ij}^{AP} = L_{ij}^{AP(RC1-RC1)} + (N-1)L_{ij}^{AP(RC1-RC2)} + \left( \frac{N}{2} - 2 \right) L_{ij}^{AP(RC2-RC2)} = \frac{3}{49} + (N-1)\frac{3}{70} + \left( \frac{N}{2} - 2 \right) \frac{3}{100}$  (18a)

$$\lim_{N \rightarrow \infty} \frac{L_{ij}^{AP}}{N} = \lim_{N \rightarrow \infty} \left\{ \frac{3}{49N} + \left( 1 - \frac{1}{N} \right) \frac{3}{70} + \left( \frac{1}{2} - \frac{2}{N} \right) \frac{3}{100} \right\} = \frac{3}{70} + \left( \frac{1}{2} \right) \frac{3}{100} \approx 0.05786 \quad (18b)$$

Figure 7(a) shows the relationship between the  $L_{ij}^{AP}$  value and the number of radical centers ( $N$ ) for models 1–3. Our AP method predicts the order of high-spin stability as “model 3 > model 2 > model 1” regardless of  $N$ . This order directly reflects the order of the increase of the  $L_{ij}^{AP}$  value per radical center, that is,  $\lim_{N \rightarrow \infty} (L_{ij}^{AP}/N)$ .

To confirm the validity of the  $L_{ij}^{AP}$  value, we compared the  $L_{ij}^{AP}$  value in this work with the  $L_{ij}^{\min(HMO)}$  value obtained by the HMO method in Figure 7(b) as the number of radical centers,  $N = 8$  and 16, are selected here. It was found that the absolute value of the  $L_{ij}^{AP}$  value is underestimated compared with the  $L_{ij}^{\min(HMO)}$  value. However, the order of the  $L_{ij}$  value for the three models exhibits a very similar

**Table 1.** Formulation of  $L_{ij}^{AP}$  Value for Models 1–3 (Two-Line System)<sup>a</sup>

(a) Model 1 <sup>b</sup>				
$N$	components of $L_{ij}^{AP}$ value			
	$L_{ij}^{AP(RC1-RC2)}$	$L_{ij}^{AP(RC2-RC2)}$	$L_{ij}^{AP(RC2-RC3)}$	$L_{ij}^{AP(RC3-RC3)}$
4	2	1	2	0
6	2	2	4	1
8	2	3	6	2
10	2	4	8	3
12	2	5	10	4
$n$	2	$(n/2)-1$	$n-2$	$(n/2)-2$

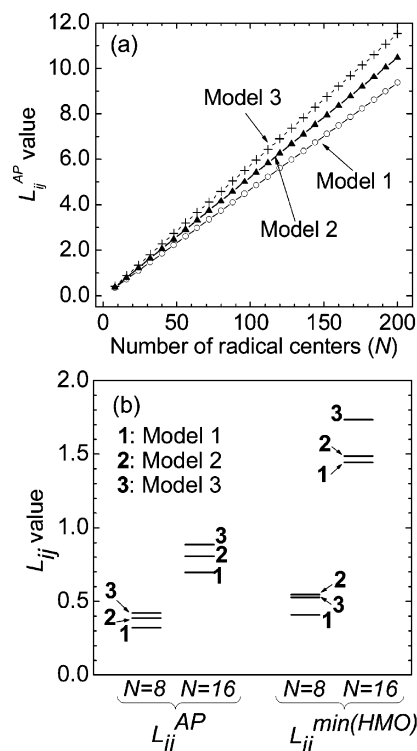
(b) Model 2		
$N$	components of $L_{ij}^{AP}$ value	
	$L_{ij}^{AP(RC1-RC2)}$	$L_{ij}^{AP(RC2-RC2)}$
4	2	3
8	2	10
12	2	17
$n$	2	$(7/4)n-4$

(c) Model 3			
$N$	components of $L_{ij}^{AP}$ value		
	$L_{ij}^{AP(RC1-RC1)}$	$L_{ij}^{AP(RC1-RC2)}$	$L_{ij}^{AP(RC2-RC2)}$
2	1	0	
4	1	3	0
6	1	5	1
8	1	7	2
10	1	9	3
$n$	1	$n-1$	$(n/2)-2$

<sup>a</sup>  $N$  represents the number of radical centers in the system.

<sup>b</sup> Systems with  $N = 4, 6$ , and 8 in model 1 are shown in Figure 6(c).



**Figure 7.** (a) Relationship between the  $L_{ij}^{AP}$  value and the number of radical centers ( $N$ ) in two-line systems (models 1–3). (b) Comparison of the  $L_{ij}$  value between the analytical prediction (AP) method ( $L_{ij}^{AP}$ ) and the HMO method ( $L_{ij}^{\min(HMO)}$ ).  $N = 8$  and 16 are selected as the number of radical centers.

tendency toward each other in both  $N = 8$  and  $N = 16$ . The only difference is the order of models 2 and 3 in  $N = 8$ . Such differences in the  $L_{ij}$  value between the AP and HMO methods result from the fact that in these models, after unitary rotation, the  $L_{ij}^{\min(HMO)}$  values do not correspond to the minimum  $L_{ij}$  value correctly, as mentioned in subsection 2.1.

Next, we examined the relationship between the  $L_{ij}^{AP}$  values and the energetic stability of the high-spin ground states ( $\Delta E(L-H)$ ) estimated by single-point calculations using ab initio MO methods by the Gaussian03 program package.<sup>25</sup> High-spin stability  $\Delta E(L-H)$  is defined as the difference in total energy between the lowest spin state ( $E(L)$ ) and the highest spin state ( $E(H)$ ), that is,  $\Delta E(L-H) = E(L) - E(H)$ . All the single-point calculations adopt the standard geometric parameters, as follows: [benzene ring] C–C = 1.395 Å, C–H = 1.100 Å; [CH or CH<sub>2</sub> group] C–C = 1.54 Å, C–H = 1.070 Å. All bond angles are fixed at 120°, and dihedral angles are fixed to keep a planar structure.

We calculated the  $\Delta E(L-H)$  values for models 1–3 at  $N = 8$  using various methods and basis sets within ab initio MO calculations (see Figure 8). The methods selected were the Hartree–Fock (HF) method, second-order Møller–Plesset perturbation theory (MP2) including frozen core (FC) approximation, and the density functional theory (DFT) method using the Becke–3–Lee–Yang–Parr (B3LYP) functional.<sup>26–28</sup> For calculating open-shell systems, we adopted the restricted open-shell Hartree–Fock (ROHF) method for each theory. The basis sets are selected as 3-21G



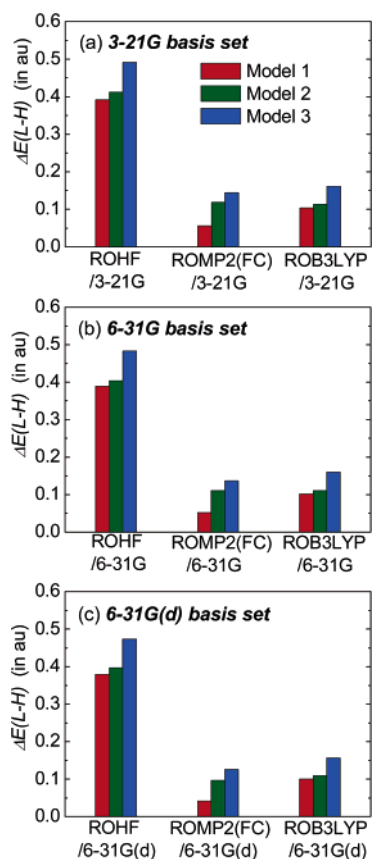


**Figure 8.** Ab initio MO calculations of high-spin stability  $\Delta E(L-H)$  for two-line systems, models 1–3 ((a) 3-21G, (b) 6-31G, and (c) 6-31G(d) basis sets).  $\Delta E(L-H)$  indicates the difference in total energy between the lowest and highest spin states, that is,  $\Delta E(L-H) = E(L) - E(H)$ .  $N = 8$  is selected as the number of radical centers.

(in panel (a)), 6-31G (in panel (b)), and 6-31G(d) (in panel (c)). Figure 8(a)–(c) shows the order of high-spin stability as “model 3 > model 2 > model 1” regardless of the method and the size of the basis set. This order of high-spin stability,  $\Delta E(L-H)$ , agrees well with the order of  $L_{ij}^{AP}$  that is predicted by our AP method. It was found from Figure 8 that the ROMP2(FC) and ROB3LYP results exhibit smaller values of  $\Delta E(L-H)$  than do the ROHF results. This is because the effects of electron correlations primarily stabilize the low-spin state. In other words, the HF calculation overestimates the stability of the high-spin state.

Furthermore, we examined the dependence of the order of  $\Delta E(L-H)$  on the number of radical centers ( $N$ ) (see Figure 9). We calculated the  $\Delta E(L-H)$  value of models 1–3 for  $N = 8, 16, 24$ , and  $32$  at the levels of ROB3LYP/3-21G. The order of high-spin stability of  $\Delta E(L-H)$  is “model 3 > model 2 > model 1” regardless of  $N$ . It was found that both the  $L_{ij}^{AP}$  value (by the AP method) and  $\Delta E(L-H)$  (by ROB3LYP/3-21G calculation) show a similar tendency in the high-spin stability of systems with even larger values of  $N$ .

**3.2. Analytical Predictions for Three-Line Systems.** In this subsection, we formulate the  $L_{ij}^{AP}$  value for the “non-disjoint closed-type” models 4–6 in three-line systems (see Figure 6(b) and Table 2). We can count the number of mixings between NBMOs in a way similar to that of the

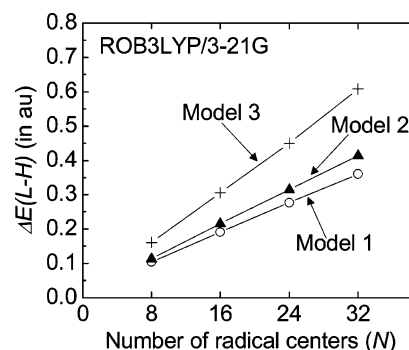


**Figure 9.** Dependence of high-spin stability  $\Delta E(L-H)$  on the number of radical centers ( $N$ ) for two-line systems (models 1–3) at the ROB3LYP/3-21G level.  $\Delta E(L-H)$  indicates the difference in total energy between the lowest and highest spin states.

two-line system. The  $L_{ij}^{AP}$  values and the increase per radical center ( $\lim_{N \rightarrow \infty} (L_{ij}^{AP}/N)$ ) for models 4–6 were estimated as

$$\begin{aligned} \text{Model 4: } L_{ij}^{AP} &= 2L_{ij}^{AP(RC1-RC2)} + \left(\frac{N}{3}\right)L_{ij}^{AP(RC2-RC2)} + \\ &\left(\frac{2}{3}N\right)L_{ij}^{AP(RC2-RC3)} + \left(\frac{4}{3}N - 7\right)L_{ij}^{AP(RC3-RC3)} = \\ &\frac{6}{70} + \frac{N}{100} + \frac{2N}{130} + \left(\frac{4}{3}N - 7\right)\frac{3}{169} \quad (19a) \end{aligned}$$

$$\begin{aligned} \lim_{N \rightarrow \infty} \frac{L_{ij}^{AP}}{N} &= \lim_{N \rightarrow \infty} \left\{ \frac{6}{70N} + \frac{1}{100} + \frac{2}{130} + \left(\frac{4}{3} - \frac{7}{N}\right)\frac{3}{169} \right\} = \\ &\frac{1}{100} + \frac{2}{130} + \frac{4}{169} \approx 0.04905 \quad (19b) \end{aligned}$$

$$\begin{aligned} \text{Model 5: } L_{ij}^{AP} &= 3L_{ij}^{AP(RC1-RC2)} + \left(\frac{N}{3} - 1\right)(2L_{ij}^{AP(RC1-RC3)} + \\ &L_{ij}^{AP(RC2-RC2)} + 2L_{ij}^{AP(RC2-RC3)}) + \left(\frac{N}{3} - 2\right)L_{ij}^{AP(RC3-RC3)} = \\ &\frac{9}{70} + \left(\frac{N}{3} - 1\right)\left(\frac{6}{91} + \frac{3}{100} + \frac{6}{130}\right) + \left(\frac{N}{3} - 2\right)\frac{3}{169} \quad (20a) \end{aligned}$$

$$\begin{aligned} \lim_{N \rightarrow \infty} \frac{L_{ij}^{AP}}{N} &= \lim_{N \rightarrow \infty} \left\{ \frac{9}{70N} + \left(\frac{1}{3} - \frac{1}{N}\right)\left(\frac{6}{91} + \frac{3}{100} + \frac{6}{130}\right) + \right. \\ &\left. \left(\frac{1}{3} - \frac{2}{N}\right)\frac{3}{169} \right\} = \frac{2}{91} + \frac{1}{100} + \frac{2}{130} + \frac{1}{169} \approx 0.05328 \quad (20b) \end{aligned}$$

$$\begin{aligned} \text{Model 6: } L_{ij}^{AP} &= 2L_{ij}^{AP(RC1-RC2)} + \left(\frac{N}{2}\right)L_{ij}^{AP(RC2-RC2)} + \\ &\left(\frac{5}{4}N - 3\right)L_{ij}^{AP(RC2-RC3)} + \left(\frac{3}{8}N - 2\right)L_{ij}^{AP(RC3-RC3)} = \\ &\frac{6}{70} + \left(\frac{N}{2}\right)\frac{3}{100} + \left(\frac{5}{4}N - 3\right)\frac{3}{130} + \left(\frac{3}{8}N - 2\right)\frac{3}{169} \quad (21a) \end{aligned}$$

$$\begin{aligned} \lim_{N \rightarrow \infty} \frac{L_{ij}^{AP}}{N} &= \lim_{N \rightarrow \infty} \left\{ \frac{6}{70N} + \left(\frac{1}{2}\right)\frac{3}{100} + \left(\frac{5}{4} - \frac{3}{N}\right)\frac{3}{130} + \right. \\ &\left. \left(\frac{3}{8} - \frac{2}{N}\right)\frac{3}{169} \right\} = \left(\frac{1}{2}\right)\frac{3}{100} + \left(\frac{5}{4}\right)\frac{3}{130} + \left(\frac{3}{8}\right)\frac{3}{169} \approx 0.05050 \quad (21b) \end{aligned}$$

Figure 10 (a) shows the relationship between the  $L_{ij}^{AP}$  value and the number of radical centers ( $N$ ) for models 4–6.

**Table 2.** Formulation of  $L_{ij}^{AP}$  Value for Models 4–6 (Three-Line System)<sup>a</sup>

(a) Model 4				
N	components of $L_{ij}^{AP}$ value			
	$L_{ij}^{AP(RC1-RC2)}$	$L_{ij}^{AP(RC2-RC2)}$	$L_{ij}^{AP(RC2-RC3)}$	$L_{ij}^{AP(RC3-RC3)}$
6	2	2	4	1
9	2	3	6	5
12	2	4	8	9
15	2	5	10	13
n	2	n/3	(2/3)n	(4/3)n-7

(b) Model 5					
N	components of $L_{ij}^{AP}$ value				
	$L_{ij}^{AP(RC1-RC2)}$	$L_{ij}^{AP(RC1-RC3)}$	$L_{ij}^{AP(RC2-RC2)}$	$L_{ij}^{AP(RC2-RC3)}$	$L_{ij}^{AP(RC3-RC3)}$
6	3	2	1	2	0
9	3	4	2	4	1
12	3	6	3	6	2
15	3	8	4	8	3
n	3	2(n/3-1)	n/3-1	2(n/3-1)	n/3-2

(c) Model 6				
N	components of $L_{ij}^{AP}$ value			
	$L_{ij}^{AP(RC1-RC2)}$	$L_{ij}^{AP(RC2-RC2)}$	$L_{ij}^{AP(RC2-RC3)}$	$L_{ij}^{AP(RC3-RC3)}$
8	2	4	7	1
16	2	8	17	4
24	2	12	27	7
32	2	16	37	10
n	2	n/2	(5/4)n-3	(3/8)n-2

<sup>a</sup>  $N$  represents the number of radical centers in the system.

From the results, our AP method predicts the order of high-spin stability as “model 5 > model 6 > model 4” regardless of  $N$ .

We calculated the  $\Delta E(L-H)$  values for models 4–6 at  $N = 24$  at the level of ROHF/3-21G and ROB3LYP/3-21G (see Figure 10(b)). Both the ROHF and ROB3LYP results predict the order of high-spin stability as “model 5 > model 6 > model 4”, although the ROB3LYP results show a smaller value for  $\Delta E(L-H)$  than do the ROHF results due to the stabilization of the low-spin state by the effects of electron correlation. Even for the three-line system, it was found that the  $L_{ij}^{AP}$  value in Figure 10(a) agrees well with the order of  $\Delta E(L-H)$  by ab initio MO calculations.

As we have seen above, it is clear that the mixing between NBMOs controls the order of the  $L_{ij}^{AP}$  value and high-spin stability. Therefore, ferromagnetic systems with large  $L_{ij}^{AP}$  values can be designed by considering the following factors.

(1) A system with strong ferromagnetic properties should involve large mixings between NBMOs such as  $L_{ij}^{AP(RC1-RC1)}$ ,  $L_{ij}^{AP(RC1-RC2)}$ ,  $L_{ij}^{AP(RC1-RC3)}$ , and so on. According to subsection 2.5, the order of magnitudes of the NBMO mixings is

$$L_{ij}^{AP(RC1-RC1)} > L_{ij}^{AP(RC1-RC2)} > L_{ij}^{AP(RC1-RC3)} > L_{ij}^{AP(RC2-RC2)} > L_{ij}^{AP(RC2-RC3)} > L_{ij}^{AP(RC3-RC3)} \quad (22)$$

(2) In a system with strong ferromagnetic properties, each NBMO should mix with many other NBMOs. For example,

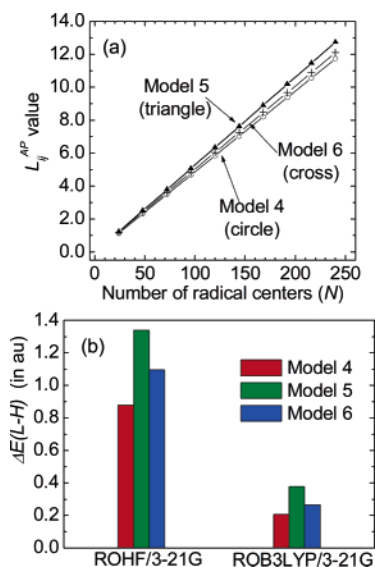


**Figure 10.** (a) Relationship between the  $L_{ij}^{AP}$  value and the number of radical centers ( $N$ ) in three-line systems (models 4–6). (b) Ab initio MO calculations of high-spin stability  $\Delta E(L-H)$  for three-line systems.  $N = 24$  is selected as the number of radical centers.  $\Delta E(L-H)$  indicates the difference in total energy between the lowest and highest spin states.

in structure A of the trimer model (see Figure 3(a)), NBMO1 mixes only with NBMO2, whereas in structure B of the trimer model (Figure 3(b)), NBMO1 mixes with both NBMO2 and NBMO3. The latter case has an advantage in the  $L_{ij}^{AP}$  value compared with the former case.

In particular, factor (1) plays a dominant role for determining the  $L_{ij}^{AP}$  value as long as we compare a similar size of oligomers. Therefore, model 3 with many  $L_{ij}^{AP(RC1-RC2)}$  and model 5 with many  $L_{ij}^{AP(RC1-RC3)}$  show the largest  $L_{ij}^{AP}$  value within the two- and three-line systems. Generally speaking, these results provide us with a few guidelines on the structure of radical units to design ferromagnetic systems with a large  $L_{ij}^{AP}$  value. First, each benzene ring should be connected to many radical centers to enlarge the  $L_{ij}^{AP}$  value. In such cases, large mixings of NBMOs are expected to generate on the benzene rings, leading to exchange interactions. Second, each radical center should not be connected to many benzene rings, because delocalized NBMOs generally provide a small  $L_{ij}^{AP}$  value due to their small NBMO coefficients.

In the present article, perfectly planar systems with no environment molecules were assumed for the simplicity. However, a deviation from the planar structure do not have primary importance for designing new materials, because it is obvious that such an effect always weakens the ferromagnetic properties due to a weakened  $\pi$ -conjugation. Indeed, the deviation effects can be easily estimated by considering overlaps between adjacent  $p$ -orbitals perpendicular to the molecular plane. Furthermore, exchange interactions through-space between environment and a target molecule is expected to be secondary effects in  $\pi$ -conjugated systems, because such through-space interactions generally show smaller effects than through-bond exchange interactions.

Although our new method was applied only to the periodic system, the method is also effective for predicting the ferromagnetism in aperiodic systems. In such cases, the  $L_{ij}^{AP}$  value is easily estimated by counting up the number of the NBMO mixings in the system.

#### 4. Conclusion

The analytical prediction (AP) method can predict the high-spin stability  $\Delta E(L-H)$  of nondisjoint closed-type benzyl radical oligomers without any direct quantum calculations. This method is composed of three procedures: (1) predicting the shape of NBMOs, (2) counting the mixings between NBMOs, and (3) formulating the relationship between the NBMO mixings and the number of radical centers ( $N$ ). Although our AP method is based on the Hückel NBMO concept for simplicity, it was confirmed that the AP method well predicts the high-spin stability evaluated by ab initio MO calculations including the post-HF method or DFT method. That is to say, our new treatment simulates higher level calculations when considering the electron correlation effects.

The AP method has the potential for predicting ferromagnetic properties in large systems. For example, formulating the NBMO mixings for periodic polymers enables qualitative prediction of the ferromagnetic properties of polymers including those involving considerably large radical units. Furthermore, the AP method can also be applied to the prediction of the ferromagnetic properties of periodic and aperiodic polymers by directly counting all the mixings between NBMOs over the whole system.

**Acknowledgment.** This work was supported by a grant-in-aid from the Ministry of Education, Culture, Sports, Science and Technology of Japan (MEXT) and by the Research and Development Applying Advanced Computational Science and Technology of the Japan Science and Technology Agency (ACT-JST). The calculations were performed on systems in our laboratory including Linux PCs.

**Note Added after ASAP Publication.** This article was released ASAP on March 30, 2006, with the incorrect Received Date. The correct version was posted on April 13, 2006.

#### References

- (1) Kinoshita, M. In *Handbook of Organic Conductive Molecules and Polymers*; Nalva, H. S., Ed.; Wiley: New York, 1997; Vol. 1, Chapter 15.
- (2) *Molecular Magnetism*; Ito, K., Kinoshita, M., Eds.; Kodansha, Gordon and Breach: Tokyo and Amsterdam, 2000.
- (3) Rajca, A. *Chem. Rev.* **1994**, *94*, 871–893.
- (4) Nishide, H.; Miyasaka, M.; Tsuchida, E. *Angew. Chem., Int. Ed. Engl.* **1998**, *37*, 2400–2402.
- (5) Rajca, A.; Rajca, S.; Wongsriratanakul, J. *J. Am. Chem. Soc.* **1999**, *121*, 6308–6309.
- (6) Rajca, A.; Wongsriratanakul, J.; Rajca, S. *Science* **2001**, *294*, 1503–1505.
- (7) Rajca, A.; Wongsriratanakul, J.; Rajca, S. *J. Am. Chem. Soc.* **2004**, *126*, 6608–6626.
- (8) Rajca, S.; Rajca, A.; Wongsriratanakul, J.; Butler, P.; Choi, S. *J. Am. Chem. Soc.* **2004**, *126*, 6972–6986.
- (9) *Magnetic Properties of Organic Materials*; Lahti, P. M., Ed.; Marcel Dekker: New York, 1999.
- (10) Sato, K.; Shimoi, D.; Takui, T.; Hattori, M.; Hirai, K.; Tomioka, H. *Synth. Met.* **2001**, *121*, 1816–1817.
- (11) Oda, N.; Nakai, T.; Sato, K.; Shimoi, D.; Kozaki, M.; Okada, K.; Takui, T. *Synth. Met.* **2001**, *121*, 1840–1841.
- (12) Michinobu, T.; Inui, J.; Nishide, H. *Org. Lett.* **2003**, *5*, 2165–2168.
- (13) Fukuzaki, E.; Nishide, H. *J. Am. Chem. Soc.* **2006**, *128*, 996–1001.
- (14) Mitani, M.; Mori, H.; Takano, Y.; Yamaki, D.; Yoshioka, Y.; Yamaguchi, K. *J. Chem. Phys.* **2000**, *113*, 4035–4051.
- (15) Dietz, F.; Tyutyulkov, N. *Chem. Phys.* **2001**, *264*, 37–51.
- (16) Huai, P.; Shimoi, Y.; Abe, S. *Phys. Rev. Lett.* **2003**, *90*, 207203.
- (17) Hagiri, I.; Takahashi, N.; Takeda, K. *J. Phys. Chem. A* **2004**, *108*, 2290–2304.
- (18) Borden, W. T.; Davidson, E. R. *J. Am. Chem. Soc.* **1977**, *99*, 4587–4594.
- (19) Borden, W. T. *Mol. Cryst. Liq. Cryst.* **1993**, *232*, 195–218.
- (20) Fang, S.; Lee, M.-S.; Hrovat, D. A.; Borden, W. T. *J. Am. Chem. Soc.* **1995**, *117*, 6727–6731.
- (21) Aoki, Y.; Imamura, A. *Int. J. Quantum Chem.* **1999**, *74*, 491–502.
- (22) Coulson, C. A.; Rushbrooke, G. S. *Proc. Camb. Phil. Soc.* **1940**, *36*, 193–200.
- (23) Longuet-Higgins, H. C. *J. Chem. Phys.* **1950**, *18*, 283–291.
- (24) Dewar, M. J. S. *J. Am. Chem. Soc.* **1952**, *74*, 3357–3363.
- (25) *Gaussian 03, Revision C.02*; Frisch, M. J.; Trucks, G. W.; Schlegel, H. B.; Scuseria, G. E.; Robb, M. A.; Cheeseman, J. R.; Montgomery, J. A., Jr.; Vreven, T.; Kudin, K. N.; Burant, J. C.; Millam, J. M.; Iyengar, S. S.; Tomasi, J.; Barone, V.; Mennucci, B.; Cossi, M.; Scalmani, G.; Rega, N.; Petersson, G. A.; Nakatsuji, H.; Hada, M.; Ehara, M.; Toyota, K.; Fukuda, R.; Hasegawa, J.; Ishida, M.; Nakajima, T.; Honda, Y.; Kitao, O.; Nakai, H.; Klene, M.; Li, X.; Knox, J. E.; Hratchian, H. P.; Cross, J. B.; Adamo, C.; Jaramillo, J.; Gomperts, R.; Stratmann, R. E.; Yazyev, O.; Austin, A. J.; Cammi, R.; Pomelli, C.; Ochterski, J. W.; Ayala, P. Y.; Morokuma, K.; Voth, G. A.; Salvador, P.; Dannenberg, J. J.; Zakrzewski, V. G.; Dapprich, S.; Daniels, A. D.; Strain, M. C.; Farkas, O.; Malick, D. K.; Rabuck, A. D.; Raghavachari, K.; Foresman, J. B.; Ortiz, J. V.; Cui, Q.; Baboul, A. G.; Clifford, S.; Cioslowski, J.; Stefanov, B. B.; Liu, G.; Liashenko, A.; Piskorz, P.; Komaromi, I.; Martin, R. L.; Fox, D. J.; Keith, T.; Al-Laham, M. A.; Peng, C. Y.; Nanayakkara, A.; Challacombe, M.; Gill, P. M. W.; Johnson, B.; Chen, W.; Wong, M. W.; Gonzalez, C.; Pople, J. A. *Gaussian, Inc.*: Wallingford, CT, 2004.
- (26) Lee, C.; Yang, W.; Parr, R. G. *Phys. Rev. B* **1988**, *37*, 785–789.
- (27) Miehlich, B.; Savin, A.; Stoll, H.; Preuss, H. *Chem. Phys. Lett.* **1989**, *157*, 200–206.
- (28) Becke, A. D. *J. Chem. Phys.* **1993**, *98*, 5648–5652.